

HGNET-BCOR Tumors of the Cerebellum

Clinicopathologic and Molecular Characterization of 3 Cases

Romain Appay, MD,* Nicolas Macagno, MD,* Laetitia Padovani, MD, PhD,†
 Andrey Korshunov, MD, PhD,‡ Marcel Kool, MD, PhD,§|| Nicolas André, MD, PhD,¶##
 Didier Scavarda, MD, PhD,** Torsten Pietsch, MD, PhD,†† and Dominique Figarella-Branger, MD, PhD*#

Abstract: The central nervous system (CNS) high-grade neuroepithelial tumor with BCOR alteration (CNS HGNET-BCOR) is a recently described molecular entity. We report 3 new CNS HGNET-BCOR cases sharing common clinical presentation and pathologic features. The 3 cases concerned children aged 3 to 7 years who presented with a voluminous mass of the cerebellum. Pathologic features included proliferation of uniform spindle to ovoid cells with fine chromatin associated with a rich arborizing capillary network. Methylation profiling classified these cases as CNS HGNET-BCOR tumors. Polymerase chain reaction analysis confirmed the presence of internal tandem duplications in the C-terminus of BCOR (BCOR-ITD), a characteristic of these tumors, in all 3 cases. Immunohistochemistry showed a strong nuclear BCOR expression. In 2 cases, local recurrence occurred within 6 months. The third case, a patient who received a craniospinal irradiation after total surgical removal followed by a metronomics maintenance with irinotecan, temozolomide, and itraconazole, is still free of disease 14 months after diagnosis. In summary, CNS HGNET-BCOR represents a rare tumor occurring in young patients with dismal prognosis. BCOR nuclear immunoreactivity is highly suggestive of a BCOR-ITD. Whether CNS HGNET-BCOR should be classified among the category of “embryonal tumors” or within the category of “mesenchymal, nonmeningothelial tumors” remains to be clarified. Because CNS HGNET-BCOR share pathologic features and characteristic BCOR-ITD with clear cell sarcoma of the kidney, these tumors may represent local variants of the same entity.

Key Words: BCOR, CNS HGNET-BCOR, BCOR-ITD methylation

(*Am J Surg Pathol* 2017;00:000–000)

The central nervous system (CNS) high-grade neuroepithelial tumor with BCOR alteration (CNS HGNET-BCOR) has recently emerged as a novel molecular entity.¹ This entity was discovered by Sturm et al¹ after molecular classification by methylation analysis of a large cohort of 323 CNS tumors institutionally diagnosed as primitive neuroectodermal tumors of the central nervous system (CNS-PNET).

Interestingly, the study by Sturm and colleagues demonstrated that up to 61% of the cases initially diagnosed as CNS-PNETs were reclassified as other well-defined molecular reference entities including mainly high-grade gliomas harboring different genetic alterations (up to 31%), and embryonal tumors (up to 18%) comprising medulloblastoma subtypes, embryonal tumors with multilayered rosettes, and atypical teratoid rhabdoid tumors.

Their study identified 4 new subgroups of CNS tumors, designated as CNS HGNET-MN1, CNS EFT-CIC, CNS NB-FOXR2, and CNS HGNET-BCOR, each harboring a distinct characteristic genetic alteration. This highlights that cases diagnosed as CNS-PNETs in the past do not correspond to a single and homogeneous molecular entity. The designation “CNS-PNET” has been removed from the recent updated fourth edition of the WHO classification of CNS tumors²; however, the 4 new molecular entities discovered in the study of Sturm et al² are not yet included in the 2016 updated WHO classification of CNS tumors. For the CNS HGNET-BCOR tumors, DNA and RNA sequencing revealed in all 10 cases studied by methylation profiling an in-frame internal tandem duplication in exon 15 of the BCOR gene (BCOR-ITD). Interestingly, the same genetic alteration has also been reported in clear cell sarcomas of the kidney (CCSKs)^{3–6} and in other very rare entities such as primitive myxoid mesenchymal tumor of infancy (PMMTI) and undifferentiated round cell sarcoma of infancy (URCSI).⁷

In this study, we report the clinicopathologic characterization of 3 new CNS HGNET-BCOR cases. They were identified by methylation profiling, polymerase chain

From the Departments of *Pathology and Neuropathology; †Radiotherapy; ‡Hematology & Pediatric Oncology; **Pediatric Neurosurgery, Timone Hospital, France; #INSERM, CRO2 UMR_S 911, Aix-Marseille Université (AMU); ‡Clinical Cooperation Unit Neuropathology; §Division of Pediatric Neurooncology, German Cancer Research Center (DKFZ); ||Cancer Consortium (DKTK), Core Center Heidelberg, Heidelberg; and ††Department of Neuropathology, Medical Center Sigmund Freud, University of Bonn, Bonn, Germany.

R.A. and N.M. equally contributed to the work.

Conflicts of Interest and Source of Funding: Supported by grants from Institut National du Cancer (grant INCa-DGOS-Inserm 6038). The authors have disclosed that they have no significant relationships with, or financial interest in, any commercial companies pertaining to this article.

Correspondence: Dominique Figarella-Branger, MD, PhD, Aix-Marseille Univ, Inserm, CRO2 UMR_S 911, 27 Boulevard Jean MOULIN, 13385, Marseille, France (e-mail: dominique.figarella-branger@univ-amu.fr).

Copyright © 2017 Wolters Kluwer Health, Inc. All rights reserved.

reaction (PCR) analysis, and immunohistochemistry showing strong BCOR expression in tumor nuclei. All 3 cases share a common clinical presentation, pathologic features, and immunoprofiles. The putative link between CNS HGNET BCOR and other tumors demonstrating BCOR tandem duplication is discussed.

MATERIALS AND METHODS

Cases were retrieved from the institutional files and material was obtained from the AP-HM tumor bank (AC 2016-1786). One case (case 1) was previously reported as cerebellar papillary meningioma.⁸ Pathology reports, all histologic sections, and available electron micrographs were reviewed. Additional immunostainings were performed on 5 µm thick formalin-fixed paraffin-embedded (FFPE) tissue sections with Ventana Benchmark XT Device. The result of conventional cytogenetic analysis of fresh tumor tissue was available in case 1. The results of comparative genomic hybridization (CGH) array were available in cases 2 and 3. Additional analyses included methylation array analysis, BCOR PCR technique, and immunohistochemical detection of BCOR protein accumulation. Information about treatment and follow-up was obtained from physicians.

Methylation Array Analysis

DNA was derived from a FFPE tumor block of each case and used for methylation analysis as previously reported.¹

BCOR Polymerase Chain Reaction

DNA was derived from representative areas of the FFPE tissue sections of each case, and sBCOR region of duplication was amplified from genomic DNA by PCR using primers BCORex16f2, TCCTCCCGCATATTCGCTG and BCORex16r, and ACACACTGTACATGGTGGTCC (35 cycles of 30 s, 94°C; 30 s, 60°C; and 80 s, 72°C). PCR products were separated on 3% agarose gels, and the aberrant bands were cut out. Extracted DNA from these gels were reamplified and sequenced.

BCOR Immunohistochemical Detection

For all 3 cases immunohistochemical detection of BCOR nuclear protein accumulation was performed on 5 µm thick FFPE tissue sections with Ventana Benchmark XT. The BCOR antibody (clone C-10 was purchased from Santa Cruz and used at 1/200 dilution).

CASE REPORTS

Case 1

This case concerned a 3-year-old boy identified with a tumor of the cerebellum after suffering for 1 month from vomiting and headaches. Magnetic resonance imaging (MRI) showed a large tumor in the posterior fossa attached to the tentorium cerebelli that was slightly enhanced after gadolinium injection. A gross total resection was performed and no adjuvant treatment was given. Local relapse occurred in October 1997; the tumor was completely removed, and local radiotherapy was undertaken. A second local relapse associated with hemispheric metastases occurred in April 1998, and chemotherapy and radiotherapy were undertaken. The patient died in October 1998 (Table 1).

Case 2

A 4-year-old boy presented with symptoms suggestive of raised intracranial pressure, including vomiting and headache. MRI revealed a large tumor in the left cerebellar hemisphere that was slightly enhanced after gadolinium injection and without any dural attachment (Figs. 1A–C). Cerebrospinal fluid analysis showed no tumor cells. Total surgical excision was performed followed by chemotherapy (VP-16 and carboplatin). Regrowth of tumor residue was observed in March 2014 that was surgically removed followed by a new line of chemotherapy. A third local relapse was recorded in May 2014, and hemicerebellectomy was performed in June 2014 followed by local radiotherapy. Local relapse and metastatic disease (bone metastases) occurred in June 2015. He died in August 2015.

Case 3

A 7-year-old girl presented after suffering from 1 month of headache and vomiting. MRI revealed a large tumor that was

TABLE 1. Clinical and Pathologic Features of the 3 Cases

Case	Sex/ Age (y)	Location	Initial Diagnosis	Extent of Surgical Removal	Postoperative Treatment	Local Recurrence and Metastatic Disease (Month After Initial Diagnosis)	Treatment of the Relapse	Outcome (mo)
1 (1997)	M/3	Cerebellum	Papillary meningioma	Total	None	LR (6) LR and MD (leptomeningeal; hemispheric) (12)	Surgery and radiotherapy Chemotherapy and spinal radiotherapy	DOD (18)
2 (2013)	M/4	Left cerebellar hemisphere	Unclassified malignant neuroepithelial tumor	Total	Chemotherapy	LR (6 and 9) LR and MD (bones metastases) (18)	Surgery and radiochemother- apy Chemotherapy	DOD (20)
3 (2016)	F/7	Right cerebellar hemisphere	Unclassified malignant neuroepithelial tumor	Total	Cranospinal irradiation and metronomic chemotherapy	None	—	FOD (14)

DOD indicates dead of disease; F, female; FOD, free of disease; LR, local recurrence; M, male; MD, metastatic disease.

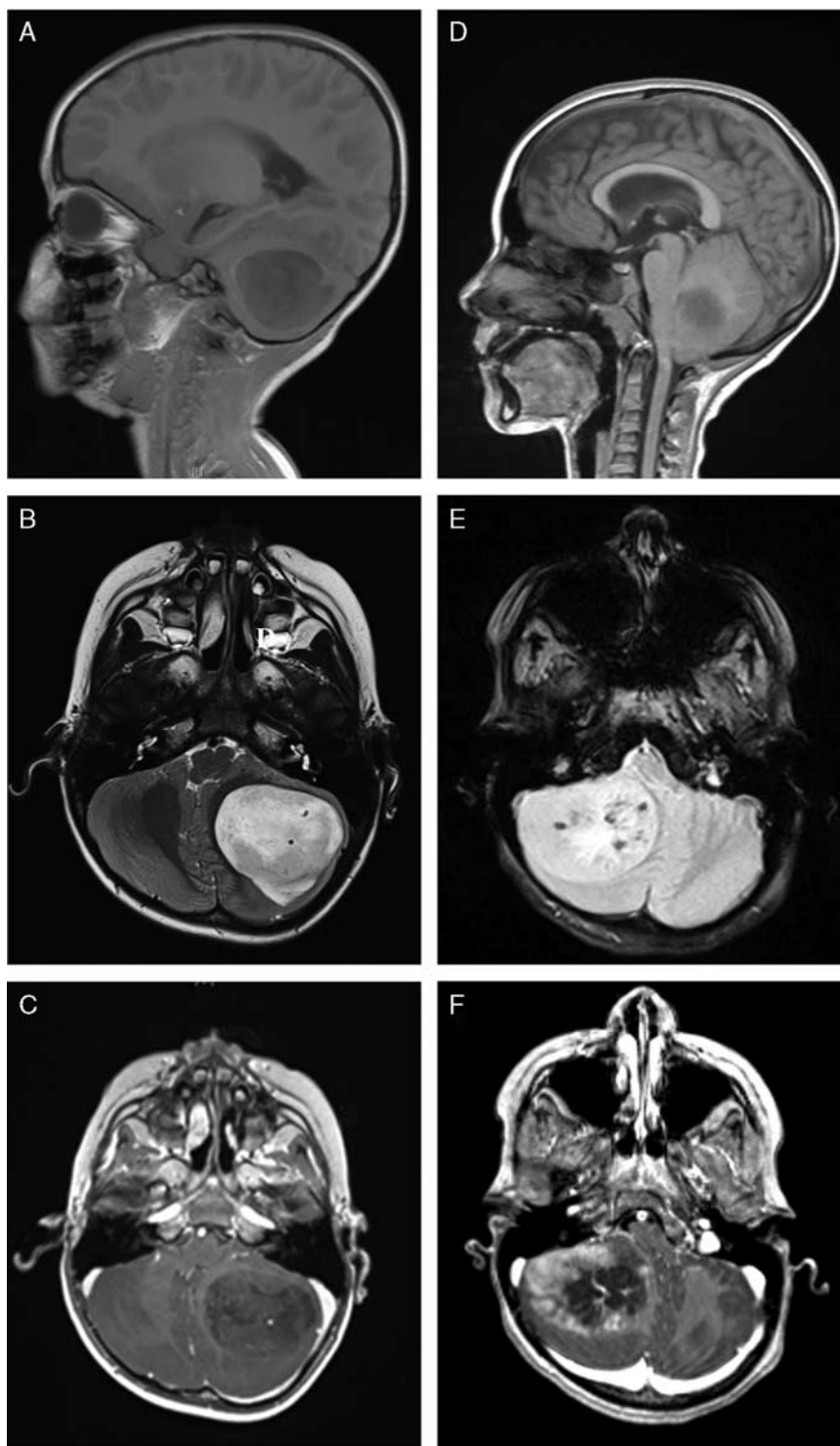


FIGURE 1. Magnetic resonance imaging of primary tumor. Case 2 (A–C) and case 3 (D–F) showed a similar large tumor located in the cerebellum, hypointense on T1-weighted sequences (A and D), hyperintense on T2-weighted sequences (B and E), and with a variable enhancement after gadolinium injection (C and F).

slightly enhanced after gadolinium injection in the right cerebellar hemisphere. The mass exhibited no attachment to the dura mater (Figs. 1D–F). Cerebrospinal fluid analysis showed no tumor cells. Total surgical excision was performed. Because pathologic

examination revealed a tumor resembling case 2, it was decided to perform craniospinal irradiation. She then received a maintenance with metronomic chemotherapy. Fourteen months after surgical resection she is still well and alive and in complete remission.

RESULTS

Pathologic Features, Karyotypic Analysis, and CGH Array Analysis

The 3 cases had similar microscopic appearance (Figs. 2A–C). Tumor cells were ovoid or fusiform with eosinophilic or clear cytoplasm. Perivascular features were a common finding, but fine fibrillary processes as usually recorded in ependymomas were lacking. The nuclei were ovoid with fine nuclear chromatin, and mitotic figures

were obvious in all cases (ranging from 4/10 high-power field in case 2, 10 in case 1 to 13 in case 3). Microcystic changes were only observed in case 2. Necrosis was recorded in cases 1 and 3 and microvascular proliferation in cases 2 and 3. Extensive immunohistochemical analyses (GFAP, Olig2, CD56, vimentin, desmin, myogenin, synaptophysin, EMA, CD34, NeuN, AE1-AE3, cytokeratin 8/18, IDH1 R132H, S100, Lin28, β -catenin, and EGFR) revealed in all 3 cases strong CD56 and vimentin immunoreactivity (Figs. 2D, E). EGFR expression was

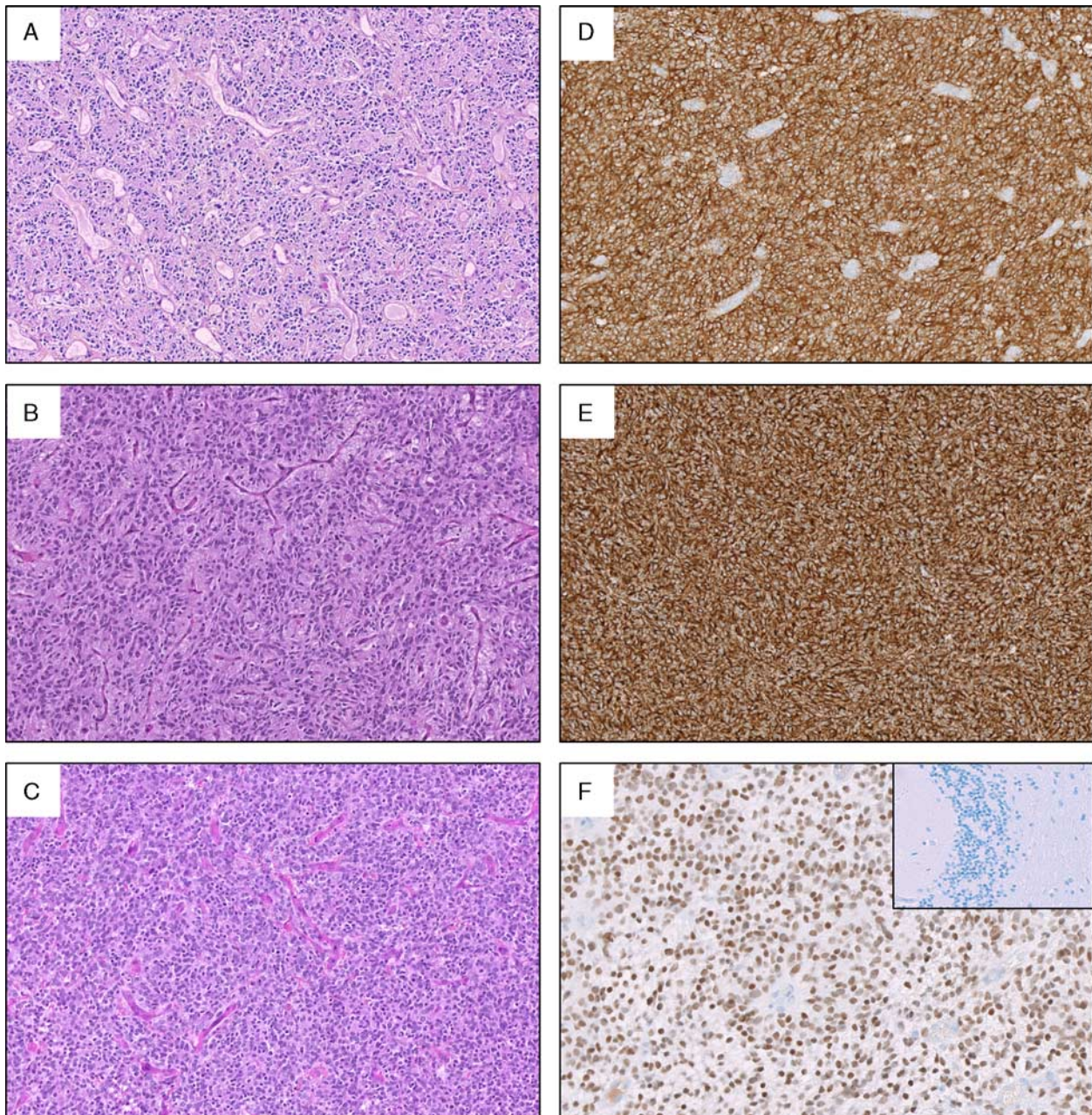


FIGURE 2. Representative histopathology of the 3 cases. Hematoxylin and eosin–stained sections exhibited similar proliferation of uniform ovoid cells with fine chromatin and a rich arborizing capillary network in case 1 (A), case 2 (B), and case 3 (C). Immunohistochemistry revealed cytoplasmic staining with NCAM (C) and Vimentin (E) antibodies and a strong nuclear staining of the tumor cells with BCOR antibody in contrast to normal cerebellum as shown in the inset (F).

recorded in 60% of tumor cells with low intensity in cases 2 and 3 but was not performed in case 1 for technical reasons. All other stainings were negative. In addition, the expression of ATRX, INI1, H3K27Me3 expression was retained. Progesterone receptor expression was faint in rare nuclei. β -catenin nuclear expression was not recorded. Reticulin did not show pericellular accumulation of argyrophilic fibers. The proliferation index was high (25% in case 2 and 40% in cases 1 and 3).

CGH array analyses, performed for cases 2 and 3, revealed no genetic alterations. Because the electron microscopy performed in case 1 revealed interdigitating cellular processes and cell junctions, a diagnosis of papillary meningioma was proposed for case 1. Cases 2 and 3 were diagnosed as “malignant neuroepithelial tumor, not classified.” We preferred this designation instead of “PNET” or medulloblastoma because pathologic features and immunohistochemical staining with lack of synaptophysin and/or LIN28 were not compatible in our experience with those diagnoses.

Assessment of HGNET-BCOR Diagnosis

Methylation Profiling

For further molecular characterization of these cerebellar tumors, we analyzed their cytogenetic and epigenetic profiles using the data generated with Illumina Methylation 450k BeadChip arrays as previously described.¹ Evaluation of 450k DNA tumor profiles disclosed no chromosomal aberrations (flat genomes) in all three cases, confirming the CGH analyses. To further evaluate molecular specificity of these tumors, we included their 450k DNA profiles in a nonsupervised hierarchical cluster analysis with methylation profiles generated for 3000 various pediatric brain tumors.

The 3 samples analyzed were clustered together with the “HGNET-BCOR” tumor cohort, confirming their molecular commonality.

BCOR-PCR Assay

In all 3 cases, we detected the expression of a larger product corresponding to the mutant (BCOR-ITD) allele in addition to normal products (Fig. 3A). Sequence analysis showed that all the abnormalities were internal tandem duplications ranging in size from 87 to 123 bp in the 3' part of the exon 15 coding sequence of BCOR. All sequence alterations were in frame and involved amino acids within the C-Terminal PUFD (PCGF Ub-like fold discriminator) domain of the protein (Fig. 3B).

BCOR Immunostaining

Anti-BCOR antibody revealed in all 3 cases strong tumor nuclei immunoreactivity (Fig. 2F). In contrast, normal cerebellum recorded in case 2 sections was negative.

DISCUSSION

The 3 cases reported here displayed similar clinico-radiologic presentation and pathologic features. Methylation analysis showed that these tumors were classified as CNS HGNET-BCOR tumors. In all 3 cases, a BCOR ITD was recorded together with a strong nuclear accumulation of BCOR protein.

All 3 cases were located within the cerebellar hemispheres, a location that was frequently encountered in the first publication, although CNS HGNET-BCOR tumors are not exclusively located in the cerebellum.¹ Because of the location and MRI findings, preoperative

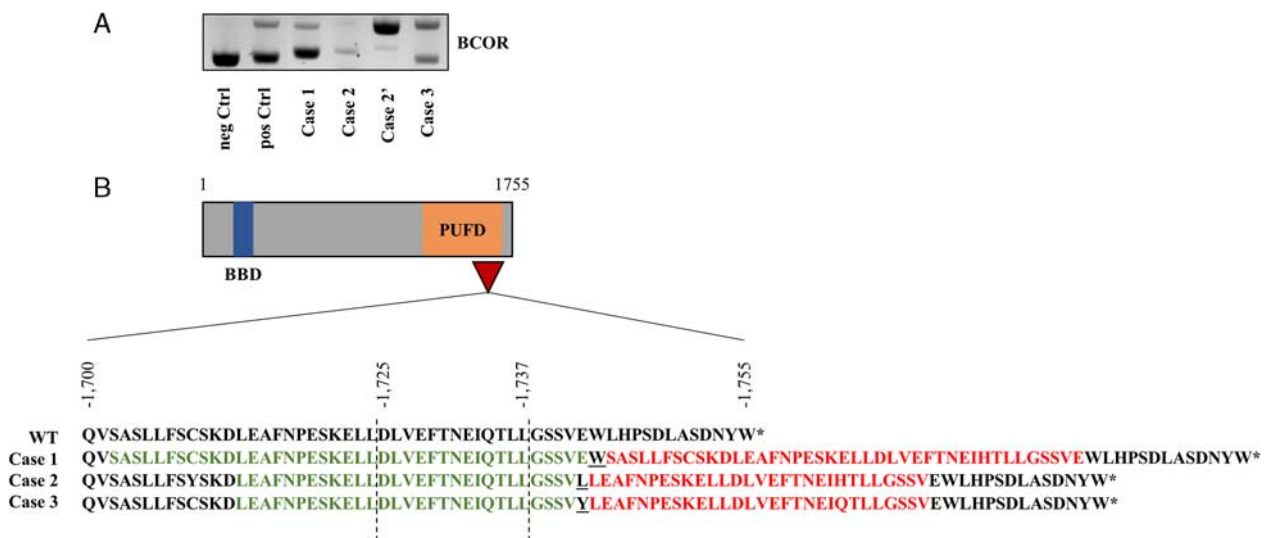


FIGURE 3. BCOR PCR assay. A, Targeted PCR of a segment of the BCOR transcript demonstrated in all 3 cases the expression of a larger product corresponding to the mutant (BCOR-ITD) allele. For case 2, because of faint bands, the extracted DNA from the gel was reamplified (case 2'). B, Schematic of predicted BCOR protein sequences from the 3 cases demonstrating the clustering of all ITDs within the C-terminal PUFD domain. Parental segments that have been duplicated are shown in green and the ITDs in red. Novel junctional amino acids (underlined) were introduced by the ITDs in all cases. A stretch of 13 residues (aa 1725-1737) is common in tumors harboring BCOR-ITD. BBD indicates BCL-6 binding domain.

diagnoses were medulloblastoma or ependymoma. Pathologic features showed in all cases a homogeneous appearance dominated by a combination of spindle to ovoid cells and frequent perivascular pseudorosettes resembling to some extent ependymomas or ETMR. In contrast to ependymomas, however, expression of GFAP and S100 was lacking. The clear cell appearance of some cells associated with lack of neuronal markers (synaptophysin, NeuN) and absence of LIN28 expression ruled out medulloblastoma or ETMR. In the first case, because of NCAM and vimentin expression and ultrastructural features compatible with meningioma, a diagnosis of papillary meningioma was initially proposed. The location of the first case in close contact with the tentorium cerebelli was compatible with this diagnosis, and lack of EMA expression, a common finding in grade III meningioma, did not rule out this presumptive diagnosis.

In all cases malignancy was obvious, assessed by high mitotic count and high proliferative index often associated with necrosis and microvascular proliferation. In keeping with the microscopic appearance, prognosis of these tumors was poor. In cases 1 and 2, local recurrence occurred within six months after surgery, and, despite surgical removal of the recurrence followed by local radiotherapy and chemotherapy, local relapse occurred again associated with metastatic disease leading to death less than two years after initial diagnosis. Because the HGNET-BCOR subgroup very often demonstrates leptomeningeal dissemination (1, this study), we strongly recommend performing spine MRI and staging the patients initially for CSF spread. Interestingly, the third case received a craniospinal irradiation followed by a metronomics maintenance with irinotecan, temozolomide, and itraconazole after total surgical removal.⁹ Fourteen months after diagnosis the girl is still free of disease. Sturm et al¹ identified several deregulated pathways in CNS HGNET-BCOR, including activation of the Sonic Hedgehog and the Wnt signaling pathway. In keeping with those findings, nuclear accumulation of β -catenin was reported,^{1,10} a feature that we did not observe. Therefore, we used a drug repositioning strategy and decided to incorporate itraconazole, which has been reported to be an Sonic Hedgehog inhibitor, in the maintenance treatment.¹¹ Interestingly, arsenic trioxide, a drug that may inhibit these pathways, reduced the viability of CNS HGNET-BCOR cells in vitro, and is another alternative drug that can be used as a potential novel therapeutic approach for patients suffering from this rare tumor.¹⁰ Of course, no conclusion can be drawn from only 1 case to recommend postoperative craniospinal irradiation in patients suffering from CNS HGNET BCOR, but this therapeutic option might be tested together with total surgical excision if feasible.

BCOR, originally reported as a BCL6 corepressor, may inhibit gene expression through its BCOR-BCL6-binding domain and potentiates the transcriptional repression of BCL6.^{12,13} Furthermore, the PUFD (PCGF Ub-like fold discriminator) domain of BCOR located at the C terminus binds to PCGF1 (Polycomb-group RING

finger homolog 1) and regulates gene transcription through an epigenetic silencing mechanism.^{14,15} BCOR ITD is also a hallmark of CCSKs.^{3,4,16} BCOR ITD consisted in the insertion of a sequence of a variable length (87 to 114bp⁴), but a shared 13-amino acid motif is always present,¹⁶ a feature also reported in CNS HGNET-BCOR^{1,10} (Fig. 3B). This common duplicated sequence is located within the PUFD domain and may facilitate tumorigenesis through aberrant epigenetic activities, but this hypothetical mechanism remains to be investigated.

Tumors harboring BCOR ITD exhibit strong expression of the protein evidenced by Western blot analysis^{1,4,10} and nuclear staining by immunohistochemistry.^{4,7} In our experience the antibody failed to detect the normal BCOR protein in the brain. This lack of immunostaining might be the consequence of a physiologically low protein expression as reported by Western blot in the kidney by Ueno-Yokohata et al³ with high protein expression in CCSK compared with the adjacent kidney. In addition, Kao and colleagues investigated the performance of this anti-BCOR monoclonal antibody (clone C-10). BCOR immunoreactivity was identified mainly in the testis but not in other normal human tissues tested such as that of the spleen, placenta, kidney, colon, liver, skin, pancreas, and lung. Furthermore, they evaluated the immunoreactivity in a large spectrum of soft tissue tumors.⁷ Most other sarcoma types tested were negative for BCOR, except 2 of 29 rhabdomyosarcomas (1 alveolar, 1 embryonal) and 1 of 92 myxofibrosarcomas, which showed moderate BCOR staining. Unexpectedly, their results revealed that half of synovial sarcomas had variable degree of BCOR immunoreactivity. The specificity of this antibody in other CNS brain tumors is unknown and deserves to be further investigated.

In addition to CNS HGNET-BCOR and CCSKs, BCOR ITD has also been reported in URCSI and in PMMTI¹⁷ (Table 2). All these tumor types occurred in young patients (infants and children) with a predominance in male patients. They usually showed a dismal prognosis and shared in common pathologic features characterized by the proliferation of uniform round or ovoid cells with fine chromatin and a rich arborizing capillary network. Additional features include stellate, vacuolated or spindle cell cytomorphology, myxoid stromal changes, and perivascular pseudorosettes.^{7,18} All these tumors displayed strong and diffuse BCOR nuclear immunoreactivity.⁷ Therefore, it is tempting to speculate that all these tumors could be different variants of the same entity. However, although CCSKs, URCSI, and PMMTI belong to the group of soft tissue tumors and are classified among sarcomas, it is unclear whether CNS HGNET-BCOR should also be classified among the category of “mesenchymal, nonmeningothelial tumors” or within the category of “embryonal tumors.”

In conclusion, CNS HGNET-BCOR represents a rare tumor occurring in young patients with dismal prognosis. Diagnosis must be considered when microscopic features mimicked to some extent ependymomas but immunostaining failed to demonstrate GFAP or EMA expression. In these

TABLE 2. Comparative Clinical Features of Tumors With BCOR Internal Tandem Duplication, Meta-Analysis

	CNS HGNET BCOR (n = 38), ^{1,9} (this study)	CCSK (n = 203) ^{3-6,14}	Infantile URCS (n = 9) ¹⁵	PMMTI (n = 6) ¹⁵
Sex (M:F)	11:8	2:1	2:1	2:1
Mean age (y)	< 10	3	< 1	< 1
Location	Cerebellum (7)	Kidney	Trunk (ST) (5)	Trunk (ST) (3)
	Parietal lobe (7)		Pelvis (ST) (2)	Abdomen (ST) (2)
	Frontal lobe (6)		Neck (ST) (2)	Neck (ST) (1)
	Temporal lobe (4)			
	Pons (1)			
	Spinal cord (1)			

F indicates female; M, male; ST, soft tissue.

cases, which strongly express NCAM and vimentin, BCOR nuclear immunoreactivity is highly suggestive of a BCOR ITD. Whether CNS HGNET-BCOR belongs to the same spectrum of other BCOR-ITD tumors or a separate entity deserves further studies.

ACKNOWLEDGMENTS

Frozen specimens from the AP-HM institution were stored and then provided by the AP-HM tumor bank (authorization number AC-2013-1786; CRB number: BB-0033-00097). Two cases have been reviewed in the RENOCCLIP network. The authors thank the associations “Sarah petite princesse” and “111 des arts” for their financial support to the RENOCCLIP network.

REFERENCES

1. Sturm D, Orr BA, Toprak UH, et al. New brain tumor entities emerge from molecular classification of CNS-PNETs. *Cell*. 2016; 164:1060–1072.
2. Louis DN, Perry A, Reifenberger G, et al. The 2016 World Health Organization Classification of Tumors of the Central Nervous System: a summary. *Acta Neuropathol (Berl)*. 2016;131:803–820.
3. Ueno-Yokohata H, Okita H, Nakasato K, et al. Consistent in-frame internal tandem duplications of BCOR characterize clear cell sarcoma of the kidney. *Nat Genet*. 2015;47:861–863.
4. Roy A, Kumar V, Zorman B, et al. Recurrent internal tandem duplications of BCOR in clear cell sarcoma of the kidney. *Nat Commun*. 2015;6:8891.
5. Karlsson J, Valind A, Gisselsson D. BCOR internal tandem duplication and YWHAE-NUTM2B/E fusion are mutually exclusive events in clear cell sarcoma of the kidney. *Genes Chromosomes Cancer*. 2016;55:120–123.
6. Astolfi A, Melchionda F, Perotti D, et al. Whole transcriptome sequencing identifies BCOR internal tandem duplication as a common feature of clear cell sarcoma of the kidney. *Oncotarget*. 2015;6:40934–40939.
7. Kao Y-C, Sung Y-S, Zhang L, et al. BCOR overexpression is a highly sensitive marker in round cell sarcomas with BCOR genetic abnormalities. *Am J Surg Pathol*. 2016;40:1670–1678.
8. Bouvier C, Zattara-Canoni H, Daniel L, et al. Cerebellar papillary meningioma in a 3-year-old boy: the usefulness of electron microscopy for diagnosis. *Am J Surg Pathol*. 1999;23:844–848.
9. André N, Carré M, Pasquier E. Metronomics: towards personalized chemotherapy? *Nat Rev Clin Oncol*. 2014;11:413–431.
10. Paret C, Theruvath J, Russo A, et al. Activation of the basal cell carcinoma pathway in a patient with CNS HGNET-BCOR diagnosis: consequences for personalized targeted therapy. *Oncotarget*. 2016;7:83378–83391.
11. Kim J, Aftab BT, Tang JY, et al. Itraconazole and arsenic trioxide inhibit hedgehog pathway activation and tumor growth associated with acquired resistance to smoothened antagonists. *Cancer Cell*. 2013;23:23–34.
12. Huynh KD, Fischle W, Verdin E, et al. BCoR, a novel corepressor involved in BCL-6 repression. *Genes Dev*. 2000;14:1810–1823.
13. Ghetu AF, Corcoran CM, Cerchietti L, et al. Structure of a BCOR corepressor peptide in complex with the BCL6 BTB domain dimer. *Mol Cell*. 2008;29:384–391.
14. Wamstad JA, Corcoran CM, Keating AM, et al. Role of the transcriptional corepressor Bcor in embryonic stem cell differentiation and early embryonic development. *PLoS One*. 2008;3:e2814.
15. Fan Z, Yamaza T, Lee JS, et al. BCOR regulates mesenchymal stem cell function by epigenetic mechanisms. *Nat Cell Biol*. 2009;11:1002–1009.
16. Kenny C, Bausenwein S, Lazaro A, et al. Mutually exclusive BCOR internal tandem duplications and YWHAE-NUTM2 fusions in clear cell sarcoma of kidney: not the full story: BCOR and YWHAE-NUTM2 changes in clear cell sarcoma of kidney. *J Pathol*. 2016;238:617–620.
17. Kao Y-C, Sung Y-S, Zhang L, et al. Recurrent BCOR internal tandem duplication and YWHAE-NUTM2B fusions in soft tissue undifferentiated round cell sarcoma of infancy: overlapping genetic features with clear cell sarcoma of kidney. *Am J Surg Pathol*. 2016; 40:1009–1020.
18. Alaggio R, Ninfo V, Rosolen A, et al. Primitive myxoid mesenchymal tumor of infancy: a clinicopathologic report of 6 cases. *Am J Surg Pathol*. 2006;30:388–394.